Nat. Hazards Earth Syst. Sci., 12, 2499–2505, 2012
www.nat-hazards-earth-syst-sci.net/12/2499/2012/
doi:10.5194/nhess-12-2499-2012

Natural Hazards and Earth System Sciences

Basal interstitial water pressure in laboratory debris flows over a rigid bed in an open channel

N. Hotta

Faculty of Life and Environmental Sciences, University of Tsukuba, 1-1-1 Tennodai, Tsukuba, Ibaraki 3058577, Japan

Correspondence to: N. Hotta (hotta.norifumi.ge@u.tsukuba.ac.jp)

Received: 31 January 2012 – Revised: 18 July 2012 – Accepted: 19 July 2012 – Published: 10 August 2012

Abstract. Measuring the interstitial water pressure of debris flows under various conditions gives essential information on the flow stress structure. This study measured the basal interstitial water pressure during debris flow routing experiments in a laboratory flume. Because a sensitive pressure gauge is required to measure the interstitial water pressure in shallow laboratory debris flows, a differential gas pressure gauge with an attached diaphragm was used. Although this system required calibration before and after each experiment, it showed a linear behavior and a sufficiently high temporal resolution for measuring the interstitial water pressure of debris flows. The values of the interstitial water pressure were low. However, an excess of pressure beyond the hydrostatic pressure was observed with increasing sediment particle size. The measured excess pressure corresponded to the theoretical excess interstitial water pressure, derived as a Reynolds stress in the interstitial water of boulder debris flows. Turbulence was thought to induce a strong shear in the interstitial space of sediment particles. The interstitial water pressure in boulder debris flows should be affected by the fine sediment concentration and the phase transition from laminar to turbulent debris flow; this should be the subject of future studies.

1 Introduction

Several models have been developed for boulder debris flows that consist mainly of a rock, gravel, and water mixture (Takahashi, 1977; Tsubaki et al., 1982; Egashira et al., 1989); sediment-laden flows (Egashira et al., 1990); or immature debris flows (Takahashi, 2007), in which an uneven sediment concentration profile forms, resulting in a lower concentration than in mature debris flows. The basic equations for these debris flows have been derived from simple modeling of the laminar motion of sediment particles, focusing on the stress structure of the particles and interstitial fluid (Takahashi, 1977; Tsubaki et al., 1982; Egashira et al., 1997). These equations have been validated experimentally, such as by comparing the theoretical and experimental velocity distributions (Takahashi, 1977; Egashira et al., 1989; Itoh and Egashira, 1999) and flow resistance (Arattano and Franzi, 2004). However, those studies did not measure the internal stress components. Few studies have succeeded in measuring the internal stresses directly; exceptions are Bagnold (1954) and Miyamoto (1985), who measured the pressure component due to particle-to-particle collisions in granular flows.

Rickenmann (1991) and Takahashi and Kobayashi (1993) investigated how increasing the fluid viscosity of clay suspensions affected the fluidity of debris flows containing coarse particles, in which the viscous coefficient of the interstitial fluid altered the total shear stress. While the excess interstitial water pressure in debris flows, including fine sediment, has been examined (Di Silvio and Gregoretti, 1997; Savage and Iverson, 2003; Iverson et al., 2010), the interstitial water pressure in boulder debris flows has often been regarded as hydrostatic. However, Egashira et al. (1989, 1997) modeled a component of the shear stresses in the interstitial fluid of boulder debris flows, in which interstitial fluid was treated as clear water, since the Reynolds stress is based on the idea that the interstitial fluid is turbulent. Although sediment particles themselves descend in a laminar motion, the interstitial fluid should be turbulent because of the strong shear induced by the sediment particles. Assuming isotropic turbulent conditions in the interstitial fluid of debris flows makes it possible to consider interstitial pressures as exceeding the hydrostatic pressure, since the Reynolds stress is the same as the shear stress. These cases imply that the interstitial water pressure in debris flows of any type should not be hydrostatic.

Iverson (1997), Imaizumi et al. (2003), and McArdell et al. (2007) succeeded in observing interstitial water pressures in excess of the hydrostatic pressure in situ or in large-scale experimental debris flows, and discussed the results in terms of liquefaction and contribution of fine sediment. Since measurements of the interstitial water pressure of debris flows under various conditions give information on the stress structure of the flows, laboratory tests are also effective. However, only a few studies have measured the interstitial water pressure in laboratory debris flows (Hotta and Ohta, 2000; Kaitna and Rickenmann, 2007; Hotta, 2011), and these have used a rotating mill (drum). Since the flow field in a rotating mill differs from that in actual debris flows due to the inherent internal flows in the rotating mill (Hotta, 2011), interstitial water pressure measurement in an open channel is preferable. Even in a laboratory setting, accurate measurements of interstitial water pressure in an open channel are difficult, because the collisions of sediment particles with the pressure gauges, especially pitot tubes, can influence the measurements. When using other types of water pressure gauges, it may also be difficult to measure the interstitial water pressure, as laboratory debris flows are usually tested in an open channel up to 10 m long (Hotta and Miyamoto, 2008). This results in a flow depth of several cm at most, so that a very sensitive pressure gauge is required to measure the interstitial water pressure. Generic water pressure gauges lack sufficient resolution at such ranges.

In this study, we developed an experimental system that uses a differential gas pressure gauge to measure the pressure in an open channel. We then measured the basal interstitial water pressure in laboratory debris flows over a rigid bed.

2 Interstitial water pressure in debris flows

The interstitial water pressure in a debris flow p_w can be expressed as follows:

$$p_\mathrm{w} = p_\mathrm{h} + p_\mathrm{f} \tag{1}$$

where p_h is the hydrostatic pressure and p_f is the Reynolds stress due to turbulent mixing in the interstitial water. The turbulence in the interstitial space of debris flows is strongly affected by particle shearing. Based on Prandtl's mixing length theory, p_f can be rewritten as

$$p_\mathrm{f} = \rho\overline{u'u'} = \rho l^2 \left(\frac{\partial u}{\partial z}\right)^2 \tag{2}$$

where ρ is the density of the interstitial water, u' is the fluctuation velocity of the interstitial water, l is the mixing length in the interstitial space, and u is the mean velocity of the interstitial water, which is assumed to correspond to the debris flow velocity. In debris flows, l is defined by the scale of the interstitial space. Ashida et al. (1985) proposed the following expression for l:

$$l = \sqrt{k_f}\left(\frac{1-c}{c}\right)^{1/3} d \tag{3}$$

where k_f is the ratio between the shape parameters for the sediment particles and the interstitial space, c is the volumetric sediment concentration, and d is the diameter of the sediment particles. Ashida et al. (1985) expressed k_f as

$$\sqrt{k_f} = \left(k_\mathrm{p}/k_v\right)^{1/3}, \quad k_\mathrm{p} = \frac{V_\mathrm{p}}{d^3}, \quad k_\mathrm{v} = \frac{V_\mathrm{v}}{L^3} \tag{4}$$

where k_p and k_v are the shape coefficients of the sediment particles and interstitial space, respectively, V_p and V_v are the unit volumes of the sediment particles and interstitial space, and L is the length scale of the interstitial space. Ashida et al. (1985) and Egashira et al. (1989) proposed values for k_f in the range 0.16 to 0.25, while Suzuki et al. (2003) reported that it was preferable to use 0.08 for k_f when a debris flow has a concentration less than 0.28. We adopted the value of 0.08 as the range of sediment concentration was no higher than 0.28 for the experiments in this study. Substituting Eq. (3) into Eq. (2) yields the following expression for p_f:

$$p_\mathrm{f} = k_\mathrm{f}\rho d^2 \frac{(1-c)^{2/3}}{c^{2/3}}\left(\frac{\partial u}{\partial z}\right)^2. \tag{5}$$

The interstitial water pressure of boulder debris flows can also be increased from the hydrostatic value in the case of different flow lines between sediment particles and interstitial water. In such a case, excess pressure is induced by an "infiltration flow" other than Reynolds stress (Hotta, 2011).

3 Experiment

3.1 Setup

The variable slope channel of the Civil Engineering Research Laboratory (904-1 Tohigashi, Tsukuba, Ibaraki, Japan) was used for the experiments (Fig. 1). The channel is 10 m long, 0.30 m wide, and 0.50 m high, with glazed sides. In this experiment, the width of the channel was restricted to 10 cm and the bottom of the lower stream of the channel (4.5 m) was raised as high as 10 cm. Sediment particles 2.9 mm in diameter were glued in the lower stream to provide bed roughness.

An ultrasonic sensor (E4PA-LS50-M1, Omron, Kyoto, Japan) was installed 1 m above the lower end to measure the temporal change in the flow surface level at a sampling rate of 20 Hz. The basal interstitial water pressure was measured at the same position. Velocity profiles were measured in some cases using a high-speed video camera.

The upper part of the channel was filled with particles to a depth of about 10 cm. A steady flow of water was supplied to

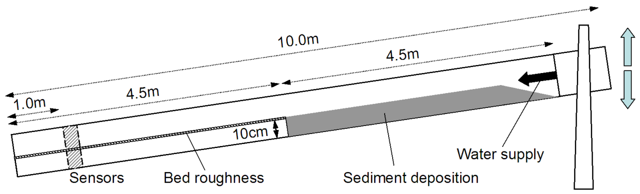

Fig. 1. Experimental setup.

Table 1. Sediment particle sizes, inclination of the open channel, and water flow rates.

Sediment particle size (mm)	Channel slope (degree)	Water supply ($\mathrm{l\,s^{-1}}$)
1.3	13	1
2.2	15	2
2.9	17	3

the upper end to generate a debris flow by eroding sediment deposits in the upper section of the channel. The debris-flow sample was captured using a sampler at the downstream end, and the sampling time was recorded. The unit width flux, Q, and the sediment flux concentration were obtained using the debris-flow sample. In this experiment system, the sediment concentration could not be controlled, as sediment was supplied only by erosion in the upper part of the channel. Because the sediment concentration fluctuated in the front section of the debris flows, the debris flow samples were obtained at the lower end of the channel during the steady-state section, which could be verified by referring to the time series of the surface level data measured by the ultrasonic displacement sensor. The average flow depth h was also obtained for the steady-state section, and the vertical (and cross-sectional) average flow velocity U_m was obtained from the following relationship:

$$Q = hU_m. \quad (6)$$

Table 1 summarizes the materials and experimental conditions. Silica sands were used in the experiments. Each sand in Table 1 was sieved using a sieve mesh of 0.8 mm and 1.4 mm, 1.4 mm and 2.0 mm, and 2.0 mm and 3.2 mm, for sediment particle sizes of 1.3 mm, 2.2 mm, and 2.9 mm, respectively. The sediment particle size in Table 1 is the mean particle size calculated from the relationship between the volume and number of sediment particles, assuming a spherical shape. The mass density and the interparticle friction angle of the sediment particles were 2.6 and 34°, respectively. The Froude numbers in the experiments ranged from 2.5 to 4.6, indicating that all flows were in a supercritical flow condition.

3.2 Measuring the interstitial water pressure

Differential gas pressure gauges (AP-47, Keyence, Osaka, Japan) were used to measure the interstitial water pressure with a sampling rate of 20 Hz. The measurement range of the AP-47 is a water depth of 0 to 20 cm, which was sufficient resolution for measuring the interstitial water pressure of laboratory debris flows in this study. Since the AP-47 cannot measure the water pressure directly, a diaphragm was attached, as shown in Fig. 2. A silicon tube with an internal diameter of 4 mm was connected to the measuring part of the gauge, while aluminum tubing with internal and external diameters of 9 and 10 mm, respectively, was connected to the opposite end of the silicon tube. A 0.03-mm-thick latex sheet was glued to the end of the aluminum tubing to act as the measurement surface. Based on a calibration with hydrostatic pressure, this sensor showed good linearity but was readily affected by temperature changes. Therefore, the air and water temperatures were monitored during the tests and compared before and after each experiment to confirm that no significant difference arose. The measurement section was located at the side wall, 1 m from the end of the channel. Measurements were taken at a height of 0 m (i.e. at the bed surface).

To avoid the direct collision of sediment particles, the measurement surface was covered with a vinyl mesh with a 0.9 mm pitch. To release the internal gas pressure relative to atmospheric before and after each experiment to initialize the measurements, a small valve was inserted between the measurement surface and the pressure gauge.

The sensor was calibrated for hydrostatic pressure by storing clear water temporarily at the measuring section, as shown in Fig. 3. The stored water was drained gradually from the measured section, and the time series of sensor signal and water depth obtained from the ultrasonic sensor were compared and calibrated. This calibration was conducted before and after each experiment. Experimental data were analyzed only when the calibrations before and after an experiment showed good agreement (Fig. 4a). When the calibration results did not correspond (Fig. 4b) or the sensor output did not show sufficient linearity (Fig. 4c), the data were eliminated. Since a slight difference in the measurement positions between the ultrasonic sensor and measurement surface of interstitial water pressure caused disagreement in the starting point of the values, zero-shift calibration was also conducted in each experiment. This calibration used the data from the final section of the laboratory debris flow (Fig. 3), where the flow consisted only of water, since the sediment in the upper part of the channel had eroded totally.

The measurement surface was replaced after several experiments due to its fragility. Ultimately, less than half of all data were suitable for analysis.

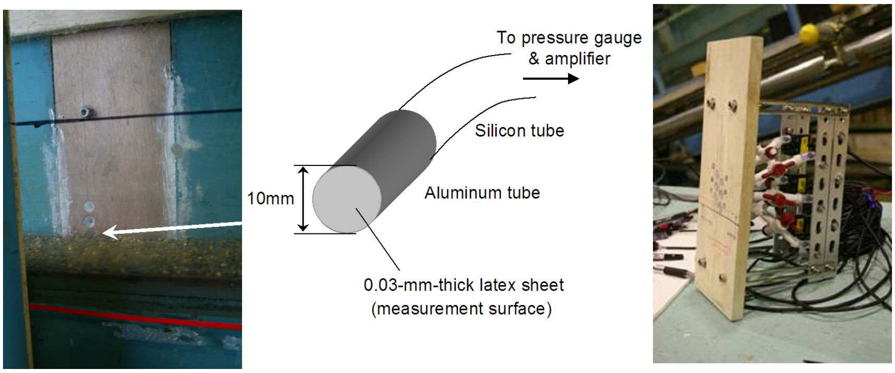

Fig. 2. Measurement system. Although several measurement surfaces are shown in the figure, only the measurement surface at the bed height was used.

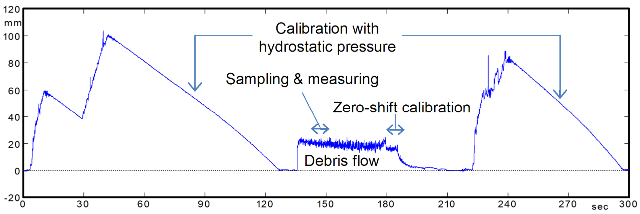

Fig. 3. Operation throughout an experiment.

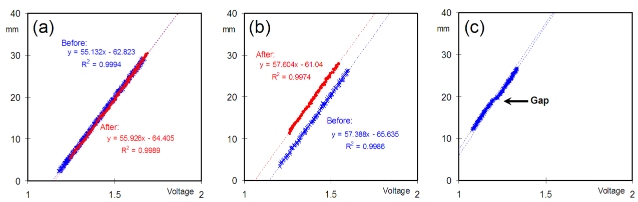

Fig. 4. Examples of **(a)** successful sensor calibration, and calibration failures due to **(b)** a difference in the pre- and post-experiment offset and **(c)** a sensitivity gap (non-linearity) during the calibration.

4 Results and discussion

4.1 Interstitial water pressure of laboratory debris flows

Figure 5 shows a time series of the flow depth and basal interstitial water pressure of the debris flow. The interstitial water pressure is expressed as a water depth (mm). Both the flow depth and interstitial water pressure fluctuated, but the debris flow exhibited an overall trend: the front part was followed by a section at steady state, and the final section showed a gradual reduction in the flow depth and interstitial water pressure. The steady-state section could be subdivided into two: the debris-flow part and the water-flow part where the flow depth decreased because of the decreased sediment volume. As shown in Fig. 5, the fluctuation of interstitial water pressure corresponded closely with that of the flow depth,

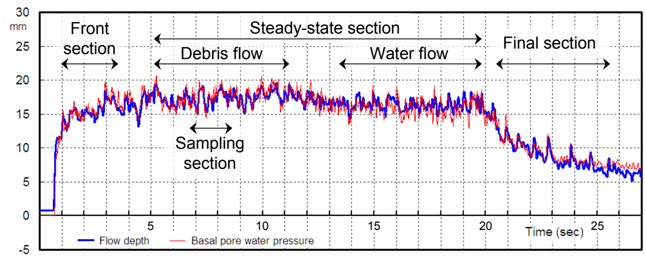

Fig. 5. Time series of flow depth and interstitial water pressure for a particle diameter of 1.3 mm, channel slope of 13°, and water supply of $2\,l\,s^{-1}$.

demonstrating an accurate sensor response, even at a high temporal resolution. The value of interstitial water pressure was in close agreement with the flow depth, indicating that the interstitial water pressure roughly equaled the hydrostatic pressure in this experimental case. Debris-flow samples were obtained during the debris-flow part in the steady-state section, as shown in Fig. 5.

Figure 6 shows the relationship between the mean flow depth and interstitial water pressure of the debris flows during the sampling period (Fig. 5) for all experiments. The line for hydrostatic pressure on which the interstitial water pressure corresponds to the flow depth is also shown. Despite using the same water supply, the flow depth (and interstitial water pressure concomitantly) differed with the sediment particle size as the flow resistance of the debris flow changed with the particle size, as predicted by the constitutive equations for boulder debris flows (Takahashi, 1977; Tsubaki et al., 1982; Tubino and Lanzoni, 1993; Egashira et al., 1997). The results indicated that the interstitial water pressure is nearly equal to or slightly greater than the hydrostatic pressure. In experiments with particle diameters of 2.9 mm, the interstitial water pressure was apparently higher than the hydrostatic pressure. Although the standard deviation hit the 1 : 1 line, the mean values were considered to be reliable. The wide range of the standard deviation of interstitial water pressure was induced

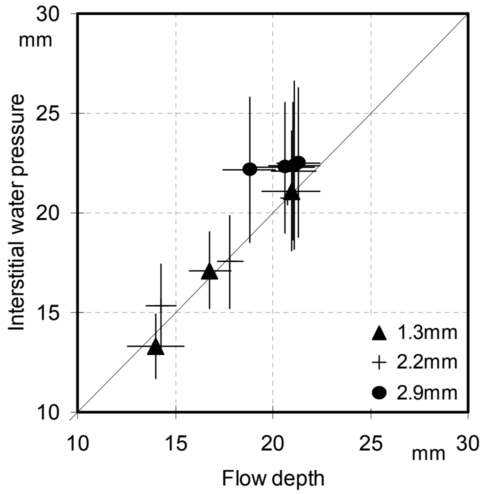

Fig. 6. Relationship between flow depth and interstitial water pressure. Mean values and standard deviations are shown. The solid line indicates the hydrostatic pressure.

mainly by the fluctuating flow depth. This was shown by the fact that the horizontal standard deviation and the interstitial water pressure gauge showed a good response to the flow depth with high temporal resolution (Fig. 5).

Table 2 summarizes the experimental results of the interstitial water pressure measurement over a series of runs. The Froude number, Bagnold number, and grain Reynolds number are also shown as reference indices.

4.2 Comparison of the measured and theoretical interstitial water pressures

First, the laminar motion of the sediment particles in the laboratory debris flows was evaluated using a high-speed video camera to confirm the assumption of the constitutive equations that express the theoretical excess interstitial water pressure as a Reynolds stress in the interstitial water of the particles. Although the velocity profile for a boulder debris flow is often given as the typical velocity profile for a dilatant fluid (Takahashi, 1977) that can be written using U_m as expressed in Eq. (7), the velocity profiles of the debris flows in the experiments appeared almost linear for the grain inertia regime (Fig. 7), like those of Tubino and Lanzoni (1993) and Armanini et al. (2005).

$$u = \frac{5}{3}U_m \left\{1 - \left(1 - \frac{z}{h}\right)^{3/2}\right\} \tag{7}$$

Differentiating Eq. (7) and substituting into Eq. (5) yields the theoretical interstitial water pressure, as Hotta (2011) showed. However, in this study, a linear velocity profile was adopted based on the experimental results (Fig. 7), and $\partial u/\partial z$ in Eq. (5) was set to

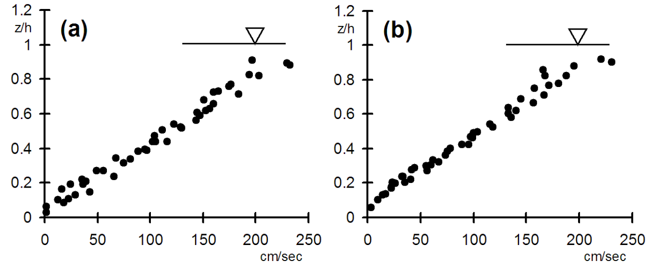

Fig. 7. Velocity profiles for experiments with channel slopes of **(a)** 13° and **(b)** 17°, with 2.9-mm sediment and a $2\,\mathrm{l\,s^{-1}}$ water supply.

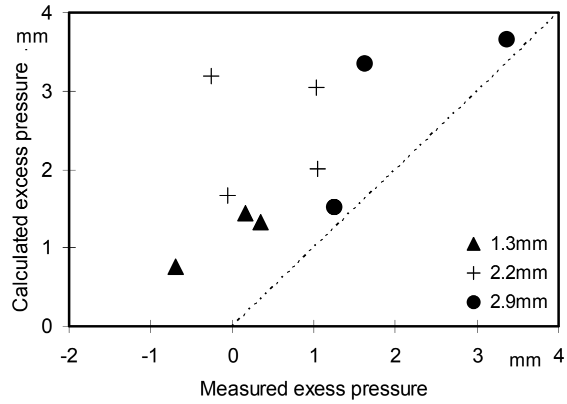

Fig. 8. Relationship between the measured and calculated values of the excess interstitial water pressure over hydrostatic pressure. The dotted line indicates the agreement between theoretical and experimental values.

$$\frac{\partial u}{\partial z} = \frac{2U_m}{h} \tag{8}$$

The theoretical value of p_f (excess hydrostatic pressure) can be derived by substituting Eq. (8) and the experimental data into Eq. (5). A uniform sediment concentration was also assumed. Consequently, a uniform p_f profile can be obtained from Eq. (5), which differs from the theoretical p_f distributions derived by Hotta and Ohta (2000) and Hotta (2011).

The theoretical and experimental values of p_f are compared in Fig. 8. The values were correlated: the theoretical p_f increased with the experimental p_f. However, the calculated values were larger than the measured values, diverging from the one-to-one line on which the theoretical and experimental values are identical (Fig. 8).

One possible cause of this disagreement is an overestimation of the theoretical p_f. When calculating the theoretical p_f, we used the experimental sediment flux concentration as c in Eq. (5). However, the sediment flux concentration differs from the volumetric sediment concentration c when the profile of c is not uniform. In an open channel, Egashira et al. (1997) pointed out that the sediment flux concentration

Table 2. Summary of interstitial water pressure measurement results.

Run No.	Channel slope (degree)	d (mm)	Q ($cm^3 s^{-1}$)	c	U_m ($cm s^{-1}$)	h (mm)	p_f (mm)	Froude number	Bagnold number	Grain Reynolds number
1	13	1.3	1437.4	0.20	102.7	14.0	13.3	2.8	1078	295
2	13	1.3	2394.0	0.14	142.5	16.8	17.1	3.5	1071	311
3	13	1.3	3556.4	0.11	170.2	20.9	21.1	3.8	935	341
4	13	2.2	1322.7	0.16	92.5	14.3	15.3	2.5	2335	489
5	13	2.2	2491.7	0.14	140.0	17.8	17.6	3.3	2720	542
6	13	2.2	3247.0	0.12	153.9	21.1	22.1	3.4	2399	582
7	15	2.2	2964.8	0.23	142.8	20.8	20.7	3.2	2979	662
8	13	2.9	2840.3	0.17	134.8	20.7	22.3	3.0	4431	782
9	17	2.9	3358.3	0.24	161.8	18.8	22.2	3.8	7075	891
10	17	2.9	4425.0	0.23	209.5	21.1	22.4	4.6	7866	936
11	15	2.9	3222.7	0.27	151.4	21.3	22.5	3.3	3427	906

falls below the volumetric sediment concentration as the sediment concentration decreases from the bed to the surface. From Eq. (5), p_f decreases with increasing c, inferring that the difference between the measured flux sediment concentration and the actual volumetric sediment concentration induces the overestimation of p_f. Although the sediment concentration profile of the debris flow on a rigid bed should be more moderate than that on an erodible bed (e.g. such as that examined by Egashira et al., 1997), the overestimation could be significant near the bed layer due to the sediment concentration profile.

Above all, the most important result in this study is the correlation between the theoretical and experimental p_f. As Fig. 8 shows, a higher p_f was measured and calculated in cases with larger sediment particles. Larger sediment particles indicate a greater mixing length from Eq. (3). This implies that the p_f of boulder debris flows increases due to the Reynolds stress with increasing mixing length in the interstitial water, where the strong shear of sediment particles induces turbulence. As shown in this study, the excess interstitial water pressure in boulder debris flow is quite low, especially when the interstitial fluid can be regarded as pure water. Although this kind of in situ debris flows can only be observed visually, measuring the interstitial water pressure under the minimum condition is important. The interstitial water pressure in debris flows with that condition will be the subject of future studies to examine, for example, the effect of increasing the fine sediment concentration and modifying the phase transition from laminar to turbulent debris flow, since the interstitial water pressure should increase and play a key role in these flows, as observed in the field.

5 Conclusions

This study developed an experimental system employing a differential gas pressure gauge to measure the basal interstitial water pressure in shallow laboratory debris flows in an open channel. The linearity and response of the manufactured sensor were validated. Although the interstitial water pressure was quite low, an increase from the hydrostatic pressure was detected with increasing sediment particle size. The measured excess interstitial water pressure corresponded to the theoretical excess interstitial water pressure, which was thought to be induced as a Reynolds stress in the interstitial water of boulder debris flows in which interstitial water is sheared strongly by the sediment particles, resulting in turbulent conditions.

Acknowledgements. I sincerely thank Mr. Miyamoto (University of Tsukuba) for his comments on this study. I also thank Mr. Sugiura and Mr. Hasegawa (Civil Engineering Research Laboratory, Ibaraki, Japan) for their help with the experiments. This research was partially supported by Grant-in-Aid for Scientific Research 17780118, 2005 and 22780140, 2010 from the Ministry of Education, Science, Sports, and Culture, of Japan.

Edited by: M. Arattano
Reviewed by: two anonymous referees

References

Arattano, M. and Franzi, L.: Analysis of different water-sediment flow processes in a mountain torrent, Nat. Hazards Earth Syst. Sci., 4, 783–791, doi:10.5194/nhess-4-783-2004, 2004.

Armanini, A., Capart, H., Fraccarollo, L., and Larcher, M.: Rheological stratification in experimental free surface flows of granular-liquid mixtures, J. Fluid Mech., 532, 269–319, 2005.

Ashida, K., Egashira, S., Kamiya, H., and Sasaki, H.: The friction law and moving velocity of a soil block on slopes, Annals of the Disaster Prevention Research Institute, Kyoto University, 28, B-2, 297–307, 1985 (in Japanese with English summary).

Bagnold, R. A.: Experiments on a gravity-free dispersion of large solid spheres in a Newtonian fluid under shear, Proc. Roy. Soc. Lon. Ser-A., 225, 49–63, 1954.

Di Silvio, G. and Gregoretti, C.: Gradually varied debris flow along a slope, Proceedings of the 1st International Conference on Debris-Flow Hazards Mitigation, San Francisco, California, 7–9 August 1997, 767–776, 1997.

Egashira, S., Ashida, K., Yajima, H., and Takahama, J.: Constitutive equations of debris flow, Annals of the Disaster Prevention Research Institute, Kyoto University, 32, B-2, 487–501, 1989 (in Japanese with English summary).

Egashira, S., Ashida, K., Takahama, J., and Tanonaka, S.: Sediment transport formula derived from an energy dissipation model of solid–fluid mixture, Annals of the Disaster Prevention Research Institute, Kyoto University, 33, B-2, 293–306, 1990 (in Japanese with English summary).

Egashira, S., Miyamoto, K., and Itoh, T.: Constitutive equations of debris flow and their applicability, Proceedings of the 1st International Conference on Debris-Flow Hazards Mitigation, San Francisco, California, 7–9 August 1997, 340–349, 1997.

Hotta, N.: Pore water pressure distributions of granular mixture flow in a rotating mill, Debris-Flow Hazards Mitigation: Mechanics, Prediction and Assessment, edited by: Genevois, R., Hamilton, D. L., and Prestininzi, A., Casa Editrice Universita La Sapienza, Roma, 319–330, 2011.

Hotta, N. and Miyamoto, K.: Phase classification of laboratory debris flows over a rigid bed based on the relative flow depth and friction coefficients, Int. J. Erosion Contr. Eng., 1, 54–61, 2008.

Hotta, N. and Ohta, T.: Pore-water pressure of debris flows, Phys. Chem. Earth. Pt. B., 25, 381–386, 2000.

Imaizumi, F., Tsuchiya, S., and Ohsaka, O.: Flow behavior of debris flows in the upper stream on mountainous debris torrent, J. Erosion Contr. Eng., 56, 14–22, 2003 (in Japanese with English summary)

Itoh, T. and Egashira, S.: Comparative study of constitutive equations for debris flows, J. Hydrosci. Hydra. Eng., 17, 59–71, 1999.

Iverson, R. M.: The physics of debris flows, Rev. Geophys., 35, 245–296, 1997.

Iverson, R. M., Logan, M., LaHusen, R. G., and Berti, M.: The perfect debris flow? Aggregated results from 28 large-scale experiments, J. Geophys. Res-Earth., 115, F03005, doi:10.1029/2009JF001514, 2010.

Kaitna, R. and Rickenmann, D.: A new experimental facility for laboratory debris flow investigation, J. Hydraul. Res., 45, 797–810, doi:10.1080/00221686.2007.9521817, 2007.

McArdell, B. W., Bartelt, P., and Kowarski, J.: Field observations of basal forces and fluid pore pressure in a debris flow, Geophys. Res. Lett., 34, L07406, doi:10.1029/2006GL029183, 2007.

Miyamoto, K.: Mechanics of grain flows in Newtonian fluid, Ph.D.-thesis presented to Ritsumeikan University, Japan, 1985 (in Japanese).

Rickenmann, D.: Hyperconcentrated flow and sediment transport at steep slopes, J. Hydraul. Eng-ASCE., 117, 1419–1439, 1991.

Savage, S. B. and Iverson, R. M.: Surge dynamics coupled to pore-pressure evolution in debris flows, Debris-flow Hazards Mitigation: Mechanics, Prediction, and Assessment, edited by: Rickenmann, D. and Chen, C. L., Millpress, Rotterdam, 503–514, 2003.

Suzuki, T., Hotta, N., and Miyamoto, K.: Influence of riverbed roughness on debris flows, J. Erosion Contr. Eng., 56, 5–13, 2003 (in Japanese with English summary).

Takahashi, T.: A mechanism of occurrence of mud-debris flows and their characteristics in motion, Annals of the Disaster Prevention Research Institute, Kyoto University, 20, B-2, 405–435, 1977 (in Japanese with English summary).

Takahashi, T.: Debris flows: mechanics, prediction and countermeasures, Taylor and Francis. Balkema, 448 pp., 2007.

Takahashi, T. and Kobayashi, K.: Mechanics of the viscous type debris flow, Annals of the Disaster Prevention Research Institute, Kyoto University, 36, B-2, 433–449, 1993 (in Japanese with English summary).

Tsubaki, T., Hashimoto, H., and Suetsugi, T.: Grain stresses and flow properties of debris flows, Proc. Jpn. Soc. Civil Eng., 317, 79–91, 1982 (in Japanese).

Tubino, M. and Lanzoni, S.: Rheology of debris flows: experimental observation and modeling problems, Exceptra, 7, 201–236, 1993.